The effect of initiation method on the size, monodispersity and shape of gold nanoparticles formed by the Turkevich method

Madeeha A. Uppal, Andreas Kafizas, Michael B. Ewing and Ivan P. Parkin*

Received (in Montpellier, France) 1st July 2010, Accepted 4th August 2010
DOI: 10.1039/c0nj00505c

The growth of gold nanoparticle (Au NP) colloids was initiated either thermally, by sonolysis, microwave (MWA) or hard ultra-violet (UVC; 254 nm) irradiation. The solutions were formulated analogous to Turkevich *et al*. and contained an auric acid gold source and different amounts of sodium tri-citrate reductant and stabiliser. A comparison of the initiation methods, using reagent solutions of equal concentration, was used to make gold nanoparticles. This showed marked differences in the final colloid, with variance in the monodispersity, size and shape of particles with initiation method. The physical size, shape and monodispersity of colloids formed were ascertained from transition electron microscopy (TEM) imaging. Properties such as average particle size and shape were directly related to changes in the surface plasmon resonance (SPR) band from UV-visible spectra. We demonstrate how a variety of simple initiation methods can be used to synthesise near monodisperse gold nanoparticles. More importantly, it is shown how the initiation method is fundamental to the eventual particle size of the resulting colloids; with sizes ranging from 11.0–11.9 nm in thermal reactions, 16.9–18.0 nm in sonolysis reactions, 11.3–17.2 nm in MWA reactions and 8.0–11.2 nm in UVC initiated reactions. Possible reaction pathways and mechanisms are put forward to explain these marked differences.

Introduction

Gold nanoparticles (Au NPs) have recently received great interest due principally to their intense and size/shape tuneable surface plasmon resonance (SPR) properties.[1] There is an abundance of literature that demonstrate the diversity of Au NPs applications; from the optical property enhancement of composite semiconductor thin-films,[2–7] bactericides,[8–10] improvements in cancer care through to DNA and single molecule detection.[11–14]

Several methods have been used to initiate colloidal gold formation, such as sonolysis,[15–18] laser ablation,[19,20] ultra-violet irradiation,[21–27] microwave assisted heating,[28–31] thermal heating[32–37] and pH mediated synthesis;[38] each with associated implications on particle size and shape. Furthermore, the variety of reductants, surfactants and growth directing media in addition to the diversity of solutions (aqueous, organic and inorganic) in which the colloids are grown is extensive. In order to investigate the effect of initiation method on the resultant properties of the colloid, a single system that is versatile to several initiation methods should be employed.

In the literature, the most commonly observed system for Au NP formation is the thermal tri-citrate reduction of auric acid in water, devised by Turkevich *et al*.[32–37] The mechanism by which the predominantly spherical particles are formed has been studied by several groups.[36,37,39] In addition, the effect on the reaction kinetics, monodispersity and eventual size of particles formed in accordance to varying the sodium tri-citrate to auric acid ratio, heating rate and temperature have also been comprehensively studied; where Au NPs ranging from ~10–100 nm in median size have been formed.[34–37,39] We have an interest in forming materials by a variety of initiation methods,[40] this has included the formation of gold colloids by a modified Turkevich synthesis.[41]

In this study, we investigate the effect of thermal heating, microwave assisted (MWA), hard ultra-violet light (UVC; 254 nm) and sonolysis treatment on the properties of the gold colloid formed by reduction of auric acid with tri-sodium citrate. We believe this to be the first instance in which UVC light has been shown to initiate gold nanoparticle growth in this system, this is to our knowledge the first comparative study of initiation methods for gold nanoparticle formation by the Turkevich method. Surprisingly near monodisperse particles could be made with a median size and distribution of sizes governed by the initiation method used.

Experimental

All reagents were purchased from Sigma-Aldrich UK unless otherwise stated. All glassware was washed with *aqua regia* and rinsed with copious amounts of deionised water before use. Four solutions of differing tri-sodium citrate ($Na_3C_6H_5O_7{\cdot}2H_2O$) concentrations and constant auric acid ($HAuCl_4{\cdot}3H_2O$) concentration were made up for each initiation method tested; labelled as Solutions A–D. Solutions were made up to a volume of 10 ml in distilled water, with masses and concentrations of reagents shown in Table 1. A set of Solutions A–D were made up each time for each initiation method tested; thermal heating, sonolysis, microwave (MWA) or hard ultra-violet (UVC) light. A table of the reaction protocol for each type of synthesis is shown in Table 2.

Department of Chemistry, University College London, 20 Gordon Street, London, UK WC1H 0AJ. E-mail: i.p.parkin@ucl.ac.uk; Fax: +44 (0)20 7679 7463; Tel: +44 (0)20 7679 4669

Table 1 Masses and concentrations of auric acid (Au source) and tri-sodium citrate (reductant/stabiliser) in 10 ml of distilled water that made solutions labelled A–D. Solutions A–D were made up each time and the reduction reaction initiated by (i) thermal heating, (ii) sonication, (iii) microwave and (iv) hard ultra-violet (UVC; 254 nm) irradiation

Solution identifier	Auric acid	Tri-sodium citrate
A	0.85 mg, 0.28 mM	0 mg, 0 mM
B	0.85 mg, 0.28 mM	2.5 mg, 0.96 mM
C	0.85 mg, 0.28 mM	5.0 mg, 1.94 mM
D	0.85 mg, 0.28 mM	10 mg, 3.88 mM

Table 2 A list of the protocol undertaken for initiating the reduction reaction of auric acid in tri-sodium citrate in solutions A–D for the formation of gold nanoparticles. Solutions were initiated by either (i) thermal heating, (ii) sonication, (iii) microwave or (iv) hard ultra-violet (UVC; 254 nm) light

Initiation method	Protocol
Thermal heating	Heated homogenously in an oil bath with a temperature controlled resistance wire (Barnstead Electrothermal 230 V/200 W) from room temperature to 100 °C. Removed from the heat after boiling for approximately 10 minutes and then allowed to cool to room temperature.
Sonolysis	Sonicated (Fischer Scientific; 35 W—1.5 l capacity) in a distilled water bath at room temperature for 60 minutes at 60 Hz and then left to stand for 24 h at room temperature.
Microwave	Microwave heated (Proline MicroChef ST22 750 W) for 3 minutes under reflux and allowed to cool to room temperature.
Hard UV light	Photo-irradiated with hard UV light (254 nm—Vilber Lourmat 2 × 8 W VL-208G-BDH/VWR Ltd) in shallow glass dishes (7 cm diameter) for 60 minutes. Lamp to sample distance was ~10 cm.

Results and discussion

A range of initiation methods was used to form gold nanoparticles from reaction of auric acid with tri-sodium citrate. This enabled a comparative study of how the size, shape, monodispersity and surface plasmon resonance (SPR) properties of the nanoparticles formed varied with thermal, sonolysis, microwaves and UVC-irradiation.

Colour changes characteristic for the formation of gold nanoparticles by citrate reduction of auric acid were observed in Solutions B–D for all initiation methods tested; with final colours ranging from light lilac to deep red (Fig. 1). No colour changes were seen in Solution A, regardless of the initiation method used. Solution A differed from Solutions B–D, as it did not contain any tri-sodium citrate reducing agent. The results showed the importance of the reducing agent in the formation of gold nanoparticles; regardless of the initiation method used.

Bright ruby-red coloured solutions were formed in MWA reactions; with more pink-purple coloured solutions formed by thermal heating and UVC initiated reactions. Initially colourless solutions were observed in sonolysis reactions after 60 minutes of sonication; however, colour began to show after leaving the solutions to stand for several hours (3–6 h) and deepened to a final dark red-purple colour after ~24 h.

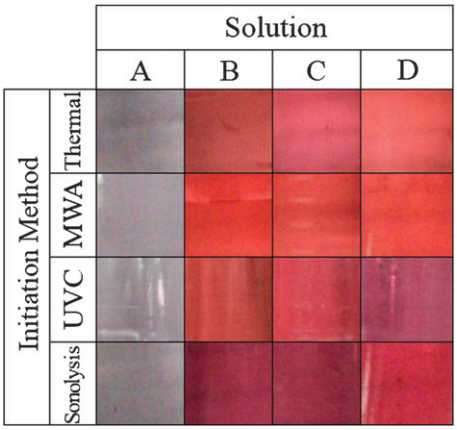

Fig. 1 Table showing the colours obtained after 24 h storage of solutions A–D; aqueous auric acid solutions with varying tri-sodium citrate concentrations after reaction by each initiation method tested (thermal heating, sonication, microwave and UVC-light). Solutions B–D all showed colour changes characteristic of colloidal gold nanoparticle formation. Solution A did not show any signs of reaction in any method tested. This demonstrated the importance of the reductant agent in the gold-nanoparticle formation mechanism, as tri-sodium citrate was not present in Solution A.

UV-visible spectroscopy

The resultant gold nanoparticle solutions from each reaction of auric acid and tri-sodium citrate (B–D for each initiation method tested) were analysed by UV-visible spectroscopy (Fig. 2) 24 h after initiation. SPR bands centred between *ca.* 519–536 nm characteristic of gold nanoparticle growth were observed in solutions B–D for all methods of initiation. Changes in the SPR band areas, heights and centres ranged from 40–91 Abs nm, 0.28–0.59 Abs units and 519–529.5 nm respectively (Table 3). This corresponds with variation in colloidal properties; such as the average nanoparticle size, monodispersity, shape and degree of agglomeration. All solutions showed a weak additional absorption band at ~260 nm. This peak relates to un-reacted auric acid, the gold source in the nanoparticle formation reactions.[36] Solutions initiated by MWA showed a more prominent absorbance at this position than any other reaction type (Fig. 2). Although this indicated that the MWA reactions were less complete than others, their average SPR band absorption height (0.47 Abs units) was of the same order as other initiation methods (0.50, 0.43, 0.51—thermal, UVC, sonolysis respectively); with values of individual solutions shown in Table 3.

It had been previously reported by Rodriguez-Gonzalez *et al*. that the gold nanoparticle formation mechanism in the thermal reduction of auric acid proceeds *via* the formation of tiny gold clusters (~1–2 nm in diameter) that bind together to form large grape like structures up to 100 nm in diameter that subsequently break apart to form the resultant colloid consisting of Au particles ~10 nm in diameter.[36,37] It was shown using titrations and electrode potential measurements that the concentration of Au(III) ions in solution decreased steadily upon boiling until complete reduction occurred.[36] These $AuCl_4^-$ ions are initially reduced by electron transfer from citrate ions to $AuCl_2^-$, which preferentially absorb excess

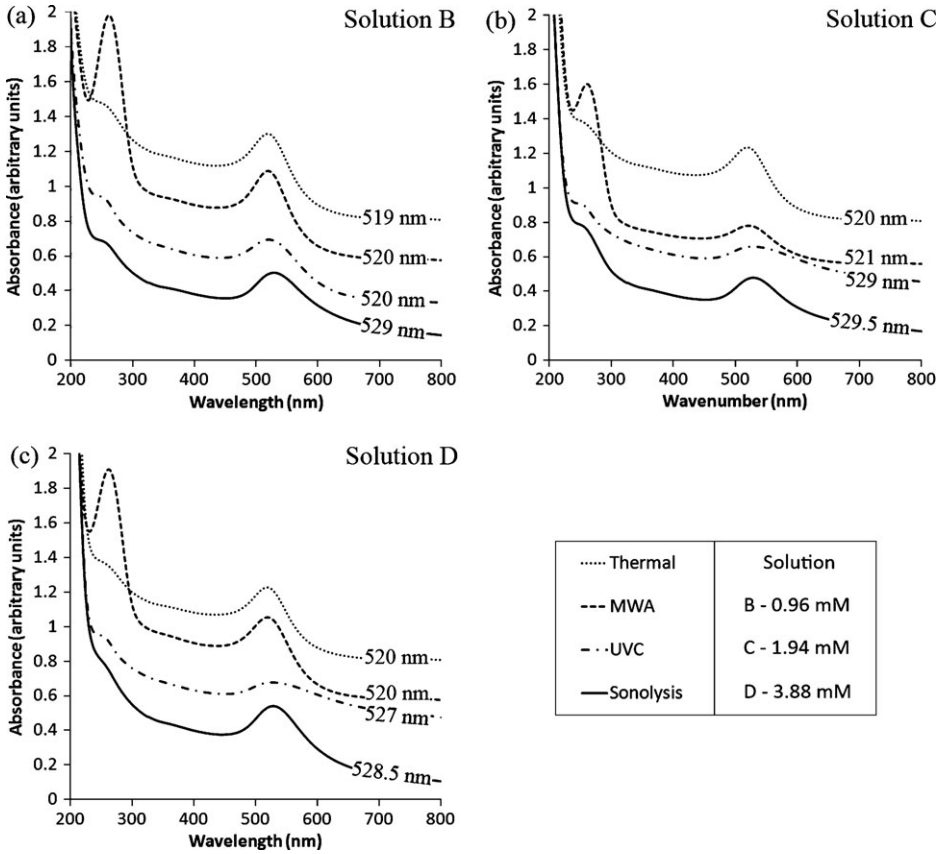

Fig. 2 UV-visible absorption spectra for gold nanoparticle solutions formed by the reduction reaction of auric acid (0.28 mM) by tri-sodium citrate of varying concentration (Solutions B–D, 0.96–3.88 mM) where the reactions were initiated by either thermal heating, sonication, MWA or UVC-light. Numbers on each profile show the position of the SPR band centre. A similarity in the absorption profiles is observed for nanoparticle solutions initiated by the same method and indicated that the method was more fundamental to the resultant colloids properties than changes in reductant concentration.

Table 3 Table of SPR band centres, absorption maxima and area from UV-visible absorption spectroscopy studies in addition to the average nanoparticle size and standard deviation error of sizes from TEM imaging of Solutions B–D (tri-sodium citrate 0.96, 1.94, 3.88 mM in B–D, respectively, auric acid consistently 0.28 mM) initiated by either thermal, MWA, UVC or sonolysis

		Surface plasmon band			TEM
		Centre/nm	Absorbance maximum	Area/Abs nm	Median Au NP size ± deviation/nm
Solution B	Thermal	519.0 (5)	0.55 (1)	65 (2)	11.4 ± 2.2
	MWA	520.0 (5)	0.59 (1)	69 (2)	17.2 ± 2.4
	UVC	520.0 (5)	0.44 (1)	65 (2)	8.0 ± 1.4
	Sonolysis	529.0 (5)	0.50 (1)	87 (2)	16.9 ± 2.1
Solution C	Thermal	520.0 (5)	0.48 (1)	58 (2)	11.0 ± 1.9
	MWA	521.0 (5)	0.28 (1)	40 (2)	11.6 ± 0.9
	UVC	529.0 (5)	0.41 (1)	87 (2)	10.8 ± 2.4
	Sonolysis	529.5 (5)	0.48 (1)	85 (2)	18.0 ± 5.0
Solution D	Thermal	520.0 (5)	0.48 (1)	57 (2)	11.9 ± 2.0
	MWA	520.0 (5)	0.56 (1)	70 (2)	11.3 ± 1.6
	UVC	527.0 (5)	0.43 (1)	91 (2)	10.9 ± 2.3
	Sonolysis	528.5 (5)	0.54 (1)	85 (2)	17.9 ± 6.1

chloride ions present in solution over citrate.[39] Excess $AuCl_4^-$ ions present in solution were continually absorbed on the surface of Au(I) particles and subsequently reduced by further citrate electron transfers. Au(I) particles continued to grow to ~1–2 nm in diameter, whilst stabilised by surrounding chloride ions. Due to their almost zero net charge, flocculation was induced and large particle clusters formed that were ~100 nm in diameter. When a saturation limit of $AuCl_2^-$ was reached, further citrate reduction produced Au atoms that ejected the surrounding chloride ions and chemisorbed with lightly bound surrounding citrate ions. This peptization process occurs rapidly, forming much smaller particles ~10 nm in diameter. Although the final colloid contains a majority of medium sized nanoparticles of around 10 nm in diameter some of the smaller

gold clusters ~1–2 nm in diameter remain. As the 1–2 nm gold clusters do not show SPR properties, being below the SPR limit, they are not detectable by UV-visible spectroscopy but can be seen in low concentration using high resolution transition electron microscopy (HRTEM).

In this study, gold nanoparticles of almost equivalent gold concentration were formed by MWA and thermal reactions as judged by the SPR band areas. However, the significantly larger presence of un-reacted auric acid seen in the UV-visible spectra (peak at ~260 nm) of MWA initiated reactions compared with thermal reactions demonstrated two major differences: (i) MWA reactions were more efficient at direct conversion of the gold source to the resultant gold colloid and (ii) the reaction possibly had a lower propensity to consume the gold source into tiny gold clusters; if the mechanism proceeded analogously to thermal reactions.

If we assume that the nanoparticle formation mechanism of MWA reactions proceeded analogously to thermal reactions, it can be deduced that more highly efficient conversion of the large grape-like intermediates to the resultant colloid occurs. However, the lower propensity for consumption of the auric acid source could not be explained. If we were to presume an alternative mechanism, whereby direct and rapid nanoparticle growth occurs at the site of a gold reduction reaction, one might explain both the reaction efficiency and higher levels of un-reacted auric acid. It is well known that MWA heating causes *in situ* rapid heating of solution pockets to occur, which may have induced the localised growth of nanoparticles, elsewhere leaving un-reacted auric acid in cooler solution packets.

In UVC-light reactions, comparatively broader SPR bands were observed (Fig. 2). This indicated a number of possibilities such as decreased monodispersity, increased particle agglomeration or changes in nanoparticle shape.[40–42] A significant red-shift in the SPR band centre from 520 nm (Solution B) to 529 nm (Solution C) was also observed for the UVC initiated reaction. The effect was attributed to the two-fold increase in the tri-sodium citrate concentration from Solution B to C. A small blue-shift to 527 nm was seen upon further increase in the tri-sodium citrate concentration; Solution D. A simple particle size control effect of the consistently increasing reductant concentration could not explain the subsequent red and blue shifts in the SPR band. TEM imaging studies later confirmed the presence of elliptical particles with varying degrees of aspect ratios, which provided an explanation for the SPR trends (Fig. 3).

Solutions initiated by sonolysis remained colourless after 1 h of sonication. A slow nanoparticle formation reaction proceeded upon leaving the solutions to stand. Initial signs of colour were observed after 6 h, which deepened in colour to a plateau after 24 h. SPR bands of the resultant colloids were red-shifted with respect to thermally activated reactions; ranging relatively invariantly from 528.5–529.5 nm. This implied the presence of significantly larger nanoparticles, which was later confirmed in TEM studies, Fig. 3. It is well documented that sonication irradiates H_2O, which generates H and OH radicals that can further initiate sonochemical reduction processes. However, Nagata *et al.* found that H radicals readily combine with atmospheric O_2 forming HO_2 radicals that compete with auric acid reduction.[43] The

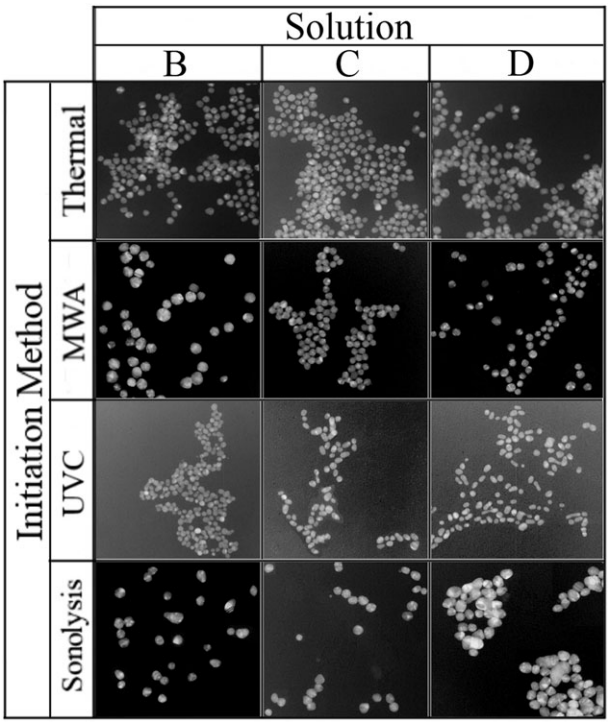

Fig. 3 TEM images (all at 100 000× magnification; image width = 300 nm) of gold nanoparticle solutions formed by the reduction reaction of auric acid (0.28 mM) by tri-sodium citrate in differing concentrations (0.96, 1.94, 3.88 mM in Solutions B–D respectively) where the reaction was initiated by either thermal heating, sonication, microwave (MWA) or hard ultra-violet (UVC) 254 nm light. Variations in the resultant nanoparticle size and monodispersity of the colloids were primarily dependent on the initiation method used, rather than the changes in the reductant concentration.

competition reaction thus provides an adequate explanation as to why Solution A did not show any evidence of colloidal gold formation in this study. Gold colloids were similarly formed by the sonication of auric acid and tri-sodium citrate solutions by Su *et al.*[18] The presence of the citrate reductant was also found to be fundamental to the formation of gold nanoparticles. H^1 NMR evidence indicated that the reduction mechanism proceeded from the removal of the OH group from tri-sodium citrate; scavenged by H radicals formed by water sonication. These tri-sodium citrate radicals subsequently reduce Au^{3+} species in solution to Au^0 and the tri-sodium citrate is re-oxidised to its original state by combining with surrounding water. Subsequent nucleation of the Au^0 atoms into larger particles is followed by capping with tri-sodium citrate stabiliser. In this study, the red coloration showing colloidal gold formation appeared several hours after sonication. Examination of the sonolysis reduction mechanism indicates a two-step process whereby the initial sonication energy induces the formation of Au^0 particles that require significant periods of time (~1 day) to fully nucleate and cap to form a stabilised colloid.

TEM imaging

The gold nanoparticles formed in Solutions B–D by each initiation method were investigated by TEM. Solution droplets were cast onto lacey carbon-coated copper grids and air-dried

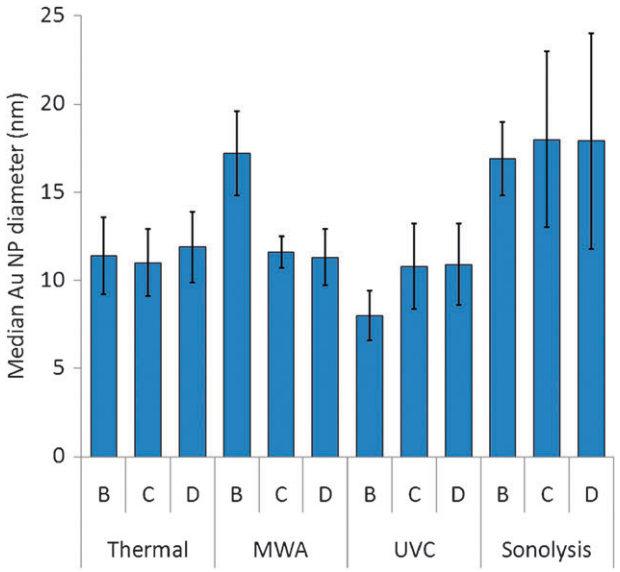

Fig. 4 Bar chart of median gold nanoparticle diameters and standard deviation errors attained from the measurement of TEM images of colloidal solutions formed by the reduction reaction of auric acid (0.28 mM) by tri-sodium citrate in differing concentrations (0.96, 1.94, 3.88 mM in Solutions B–D respectively) where the reaction was initiated by either thermal heating, microwave (MWA), hard ultra-violet (UVC) 254 nm light or sonication.

before analysis. All Solution A reactions showed no sign of nanoparticle growth; this corresponded with the absence of a colour indicating no SPR band (Fig. 1). This verified the importance of the tri-sodium citrate reducing agent for inducing nanoparticle growth, irrespective of the initiation source used in this study. Representative images of all colloids formed are shown in Fig. 3. Median and standard deviations in the measured nanoparticle diameters, from sets of at least 70–100+ measured particles, are shown graphically in Fig. 4 with values additionally listed in Table 3.

Thermally initiated reactions showed almost invariant average particle size (11.0–11.9 nm) and monodispersity (1.9–2.2 nm standard deviations) with an increased tri-sodium citrate concentration from 0.96 mM in Solution B to 3.88 mM in Solution D. This supported the UV-visible absorption

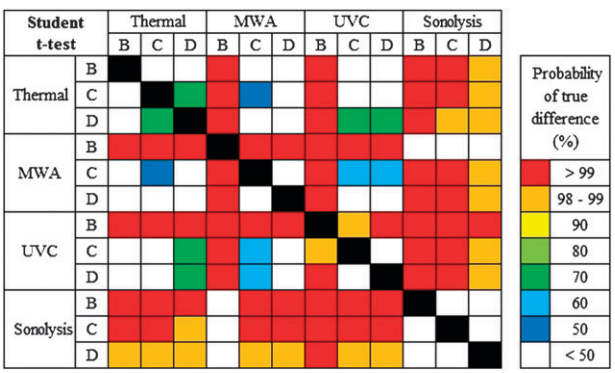

Fig. 5 A colour coded table of probable difference in the average nanoparticle size using sizes determined from TEM images by Student *t*-testing. Colours represent different probabilities of significant difference; represented in the corresponding colour-key.

studies, where no significant change in position, width or height of the SPR band was observed (Table 3). Student *t*-tests (Fig. 5) showed that the average nanoparticle size in Solution B (11.4 nm) had little chance of being significantly different from either Solutions C (11.0 nm) or D (11.9 nm); indicating equivalence (less than 1%). Within the tri-sodium citrate concentration range tested, little effect on the resulting colloid was seen. The results demonstrated the independence of average particle size and monodispersity of thermal colloid growth to the citrate concentration; within the 0.96–3.88 mM range experimentally tested.

Contrary to thermal reactions, TEM images of Solutions B–D initiated by MWA radiation showed a transition from larger nanoparticles formed in Solution B from 17.2 nm diameter on average to significantly smaller particles in Solutions C and D with 11.6 and 11.3 nm in average diameter. The monodispersity of all solutions was high, with relatively low standard deviations ranging from 0.9–2.4 nm. In contrast to what was seen in thermally initiated reactions, a concentration dependence of the tri-sodium citrate reductant was observed; where doubling the tri-sodium citrate concentration from 0.96 mM to 1.94 mM yielded smaller particles. A further increase in the reductant concentration from 1.94 mM (Solution C) to 3.88 mM (Solution D) did not form smaller particles. Student *t*-tests showed that the probability that Solution B was different from Solutions C and D was 99.9%; verifying the differences observed statistically (Table 3) and by eye (Fig. 3). The *t*-tests also showed that Solutions C and D were most likely equivalent.

Solutions initiated by UVC-light were not only relatively monodisperse but showed lower average particle sizes; with the lowest average size seen in Solution B at 8.0 nm. However, the colloids became increasingly more elliptical in shape with increased tri-sodium citrate concentration as seen by close-up images in Fig. 6. Measurement of the size aspect ratios of particles quantified the differences observed. Solution B, containing the lowest tri-sodium citrate concentration, yielded the most spherical particles with an average size aspect ratio of 1.08 ± 0.07. Increased citrate concentrations lead to increases in the elliptical nature of particles, with 1.96 mM Solution C and 3.88 mM Solution D showing size aspect ratios of 1.37 ± 0.26 and 1.56 ± 0.56 respectively. These disparities in shape might explain the unconventionally large shifts in the SPR band with little change in average nanoparticle size (Fig. 2).[40] Student *t*-tests showed that Solutions C (10.8 ± 2.4 nm) and D (10.9 ± 2.3 nm) could not be said to be significantly different from all other solutions made in this study; however it was 99.9% probable that Solution B (8.0 ± 1.4 nm) was significantly smaller in average nanoparticle size than all other colloids.

Nanoparticles initiated by sonolysis were significantly larger on average than particles formed by thermal, MWA and UVC-light. Average particle sizes ranged from 16.9 to 18.0 nm. Although the colloids showed generally lower degrees of monodispersity (Table 3), Student *t*-tests confirmed that they were significantly different (by >98% chance) than all other colloids formed, bar one, MWA—Solution B. The average red-shift in the SPR band by ~9 nm on average of sonicated solutions compared with thermally initiated solutions was

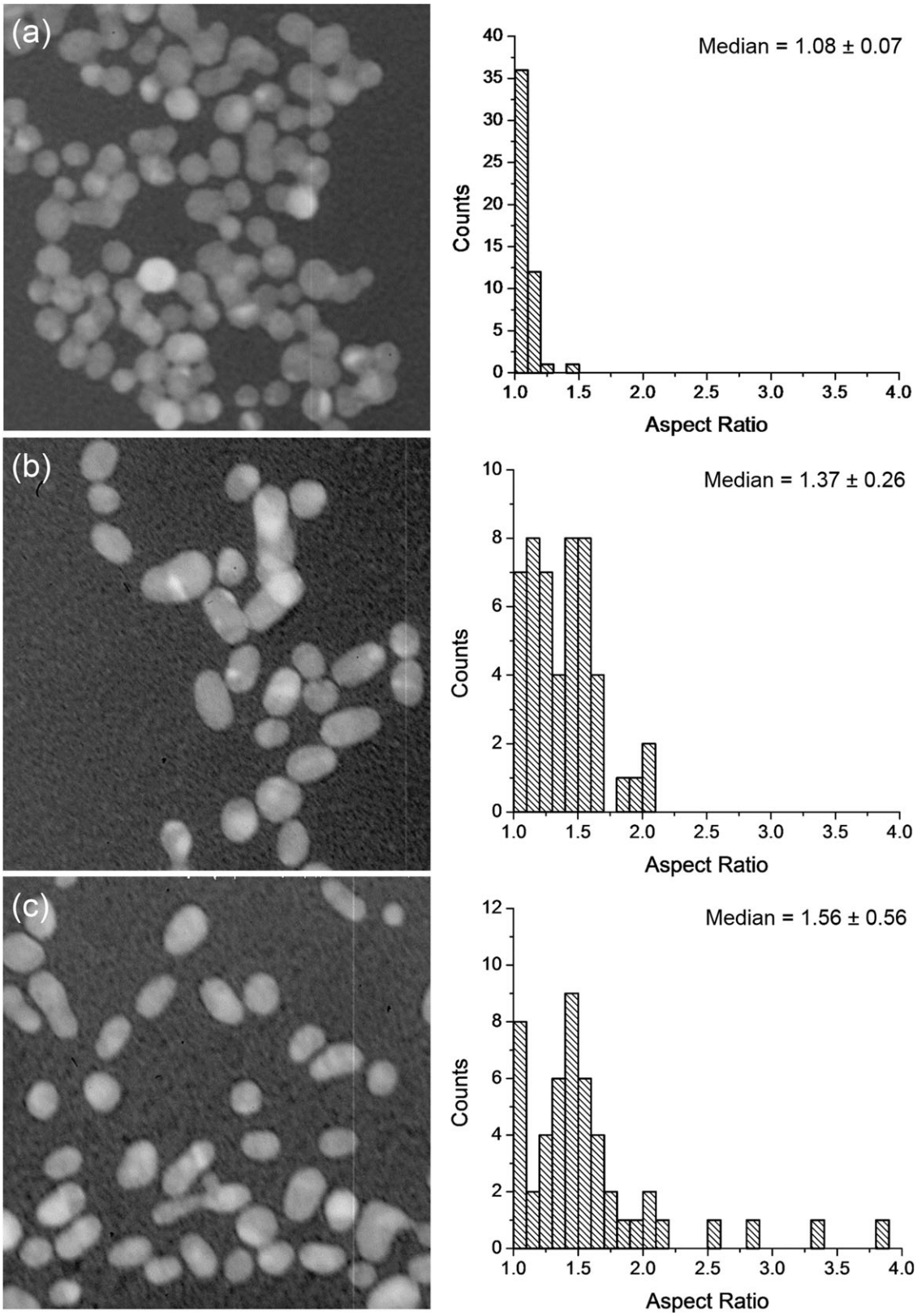

Fig. 6 Close up TEM images (All at 100 000× magnification; image width = 130 nm) of gold nanoparticle solutions formed by the reduction reaction of 0.28 mM auric acid with tri-sodium citrate of varying concentration (a) 0.96 mM, (b) 1.94 mM and (c) 3.88 mM initiated by hard ultra-violet (UVC) 254 nm light. Histogram plots of the variation in size aspect ratio of the elliptical nanoparticles are adjacently plotted, with median and standard deviations quoted.

Table 4 A table of synthetic conditions and average colloidal gold sizes including errors (nm) used by other groups compared in this study who have similarly reduced aqueous auric acid solutions with tri-sodium citrate by initiation with thermal heating, microwave (MWA), soft ultra-violet (UVC) 366 nm light and sonication

Initiation method	Concentrations/mM		Average Au NP diameter ± error/nm	Reference
	Auric acid	Tri-sodium citrate		
Thermal (100 °C, 5 min)	0.25	0.20, 0.38, 1.96	25 ± 5, 18 ± 4, 14 ± 2	Turkevich *et al.*[32]
MWA (125 °C, 80 °C min^{-1}, 600 W, 15 min)	1.0	0.9, 2.2, 3.5, 6.0, 7.5	75 ± 8, 22 ± 2, 20 ± 2, 18 ± 1.5, 25 ± 5	Liu *et al.*[31]
Sonolysis (4 °C, 20 kHz, 15–30 min)	0.49	1.9, 2.9, 3.9	18.9–19.4, 18.4–20.9, 16.9–22.0	Su *et al.*[18]
UVA (366 nm, 1 mW cm^{-2}, 2 h)	2.0	2.0	30–70 (median ~60)	Kimling *et al.*[33]

complemented by an average increase in particle size by ~6 nm in diameter. This was in contrast with UVC and MWA initiated solutions where little correlation between the SPR band centre and average nanoparticle size was observed.

Previous work by Turkevich *et al.*[32] not only established the nucleation and growth process of colloidal gold by thermal reduction of auric acid with tri-sodium citrate, but also investigated the effect of adjusting reductant concentration, gold concentration and temperature. With the auric acid concentration kept constant at 0.25 mM, a range of tri-citrate concentrations from 0.20 to 0.38 to 1.96 mM were investigated forming average nanoparticle sizes of 25 ± 5, 18 ± 4 and 14 ± 2 nm respectively (Table 4). In our work the solutions were of almost equivalent concentration to one of those formulated by Turkevich *et al.*, with Solution C consisting of 0.28 mM auric acid and 1.96 mM tri-sodium citrate. In the thermal reduction reaction in this study, Solution C formed gold nanoparticles 11 ± 2 nm in size, whilst the almost analogous reaction by Turkevich *et al.* quite similarly formed nanoparticles 14 ± 2 nm in size. The slight variation in average size could be attributed to a number of differences in experimental procedure. For instance, it was recently shown that inverse Ostwald growth of gold nanoparticles synthesised by the Turkevich method can occur if not fully heated beyond a point of full nanoparticle size evolution.[33] The double difference in initiation time could attribute to this size discrepancy. In addition, Turkevich *et al.* added tri-sodium citrate to a boiling auric acid solution whilst in this study the auric acid and tri-sodium citrate were heated together from room temperature.

However, colloids made by Turkevich *et al.* were spherical and relatively monodisperse, analogous to gold nanoparticles formed by thermal heating in this study. Yet Turkevich *et al.* witnessed significant changes in average nanoparticle size upon varying the tri-sodium citrate concentration. The average nanoparticle size increased from 14 to 25 nm upon a factor of 10 change in the tri-sodium citrate concentration from 1.96 mM to 0.20 mM. In this study, the tri-sodium citrate concentration was varied by a factor of 2 and did not yield significant changes in the average nanoparticle size for thermally initiated reactions. Combining results it becomes clear that order of magnitude changes in the tri-sodium concentration are required for significant changes in average nanoparticle size of the resultant colloid to be observed.

Gold nanoparticles formed by the tri-sodium citrate reduction of auric acid were also initiated by microwave radiation in the work reported by Liu *et al.*[31] A wide range of tri-sodium citrate concentrations were examined; from 0.9 mM to 7.5 mM solutions with the auric acid solution kept consistent at 1 mM; almost four times more concentrated than in solutions formulated in this study. The average nanoparticle size of the resulting colloid was dependent upon the tri-sodium citrate concentration with a similar trend to results from this study. Liu *et al.* observed a sharp decrease in average nanoparticle size from 70 ± 8 nm to 20 ± 2 nm upon increasing the citrate concentration from 0.9 mM to 2.2 mM. Further increases in the reductant concentration from 2.2 mM to 6.0 mM yielded no further change in colloidal particle size. A similar dependency was observed in this study, where an increase in tri-sodium citrate concentration from 0.96 mM to 1.96 mM yielded an initial decrease in average nanoparticle size from 17 ± 2 nm to 12 ± 1 nm with a further increase in reductant concentration causing no significant change (3.88 mM, 11 ± 2 nm). Although both sets of colloids formed by MWA initiation were highly monodisperse and spherical, contrasting differences in average nanoparticle size were observed and could be attributed to a number of factors; for instance the microwave used by Liu *et al.* was 25% less powerful and solutions were irradiated for only 3 minutes in our study compared to the 15 minutes by Liu *et al.*[31] In light of the work conducted by Turkevich *et al.*[32] that established the high dependency of the tri-sodium citrate/auric acid concentration on the resultant average nanoparticle size, the contrasting size differences between microwave initiated reactions in our study and that of Liu *et al.*[31] could be attributed to the consistent factor of four difference in the auric acid concentration; with 0.28 mM used in our study and 1 mM used in their work.

Work conducted by Su *et al.*[18] utilised sonolysis to induce nanoparticle formation from auric acid and tri-sodium citrate. A range of citrate concentrations from 0.49 mM to 3.9 mM were examined with the auric acid concentration kept constant at 0.49 mM. Lower levels of tri-sodium citrate from 0.49 mM to 1.5 mM caused large nanoparticle clumps to form upon sonication, ranging in size from 100–400 nm. Increasing levels of sonication lead to the formation of spherical and monodisperse colloids 17–22 nm in average diameter with a small size deviation of 1–2 nm. Although no particle clumping was seen in colloids formed by sonolysis in our study, there were several differences in experimental procedure. For instance, Su *et al.* ice-cooled their solutions to 4 °C with sonication at a frequency of 20 000 Hz whilst reactions in this study were conducted at room temperature at a much lower sonication frequency of 60 Hz. Additionally, solutions formulated by Su *et al.* contained approximately double the gold content compared with our work. In comparing the effect of the

tri-sodium citrate : auric acid ratio upon the resultant average nanoparticle size, Su *et al*. demonstrated little change over the 3 : 1 to 8 : 1 citrate : auric acid regime with particles formed 17–22 nm in average size.[18] In our study, a 3.5 : 1 to 14 : 1 citrate : auric acid regime was investigated with particles ranging quite similarly in average size from 17–18 nm. Although a sonication frequency orders of magnitude more powerful was used by Su *et al*. and a length of initiation up to four times longer was used in this study, the resultant gold nanoparticle sizes of similar reagent solutions compared well.

Hard UVC irradiation was used to initiate the formation of colloidal gold from solutions of auric acid with a tri-sodium citrate reductant. We believe this to be the first instance in which UVC light (254 nm light) has induced nanoparticle formation from this set of reagents, however, Kimling *et al*. demonstrated this process could be also induced by UVA (365 nm light) irradiation previously.[33] A comparatively larger auric acid concentration of 2.0 mM with a similar level of tri-sodium citrate was used by Kimling *et al*., which leads to the formation of colloidal gold with a larger size distribution ranging from 30–70 nm and nanoparticles ~60 nm in average diameter. Far smaller and more monodisperse colloids were formed in this study ranging 8–11 nm in average size with deviations of 1–2 nm. The elliptical nature of nanoparticles formed in this study was also not seen by Kimling *et al*. Nonetheless, higher levels of tri-sodium citrate : auric acid were used in this study ranging from 3.5 : 1 to 14 : 1 compared with a 1 : 1 ratio used by Kimling *et al*., where the increasing reductant concentration had a profound effect in increasing the elliptical nature of particles formed here.

Although several groups have individually investigated the thermal, sonolysis, microwave and UV initiated formation of colloidal gold from auric acid and tri-sodium citrate, a range of differing gold and reductant concentrations were used. The lack of consistency made fair comparisons of the method's effect on the resultant average nanoparticle size, shape and monodispersity not possible. By testing equivalent sets of solutions over a range of tri-sodium citrate concentrations we were able to observe the contrasting differences the initiation method had upon the resulting colloid.

Conclusion

Nearly monodisperse gold nanoparticle colloids were formed by a variety of initiation methods (thermal, microwave assisted, hard ultra-violet light and sonication) for a range of solutions that contained a constant concentration of auric acid (0.28 mM) and varying concentrations of tri-sodium citrate (0–3.88 mM). Gold nanoparticle solutions did not form unless tri-sodium citrate was present, regardless of the initiation method used. When the reductant was present, monodisperse gold nanoparticle formation occurred in every case. Nanoparticle solutions formed in the presence of reductant by the tradition thermal method devised by Turkevich *et al*.[32–37] were not affected by citrate concentration increases and formed colloids 11.0–11.9 nm in average size. Gold nanoparticles formed in sonolysis reactions were also unaffected by citrate concentration increases and formed larger colloids 16.9–18.0 nm in average size. Microwave assisted reactions were concentration dependent at 0.96 mM, forming nanoparticles 17.2 nm in size and yielded smaller nanoparticles with increased citrate concentrations 11.3–11.6 nm in size. Hard ultra-violet light initiated reactions formed typically smaller nanoparticles, 8.0–10.9 nm in average size, with particles more elliptical in nature. In this study, the independence to citrate concentration over the 0.96 mM to 3.88 mM range was shown; with one exception. By simply changing the initiation method, one can create monodisperse gold nanoparticle colloids with significantly varying average size (8.0–18.0 nm).

References

1 G. Walters and I. P. Parkin, *J. Mater. Chem*., 2009, **19**, 574; K. Yong, M. T. Swihart, H. Ding and P. N. Prasad, *Plasmonics*, 2009, **4**, 79.
2 M. C. Ferrara, L. Mirenghi, A. Mevoli and L. Tapfer, *Nanotechnology*, 2008, **19**, 365706.
3 L. Armelao, D. Barreca, G. Bottaro, A. Gasparotto, C. Maccato, C. Maragno, E. Tondello, U. L. Stangar, M. Bergant and D. Mahne, *Nanotechnology*, 2007, **18**, 375709.
4 A. Ito, H. Masumoto and T. Goto, *Mater. Trans., JIM*, 2003, **44**, 1599.
5 R. G. Palgrave and I. P. Parkin, *Chem. Mater*., 2007, **19**, 4639.
6 R. G. Palgrave and I. P. Parkin, *J. Am. Chem. Soc*., 2006, **128**, 1587; R. G. Palgrave and I. P. Parkin, *Gold Bull*., 2008, **41**, 66.
7 R. Binions, C. Piccirillo, R. G. Palgrave and I. P. Parkin, *Chem. Vap. Deposition*, 2008, **14**, 33.
8 S. Nath, C. Kaittanis, A. Tinkham and J. M. Perez, *Anal. Chem*., 2008, **80**, 1033.
9 J. Gil-Tomas, S. Tubby, I. P. Parkin, N. Narband, L. Dekker, S. P. Nair, M. Wilson and C. Street, *J. Mater. Chem*., 2007, **17**, 3739.
10 S. Perni, C. Piccirillo, J. Pratten, P. Prokopovich, W. Chrzanowski, I. P. Parkin and M. Wilson, *Biomaterials*, 2009, **30**, 89.
11 C. Yu, H. Nakshatri and J. Irudayaraj, *Nano Lett*., 2007, **7**, 2300.
12 M. Li, Y. Lin, C. Wu and H. Liu, *Nucleic Acids Res*., 2005, **33**, 184.
13 X. Qian and S. M. Nie, *Chem. Soc. Rev*., 2008, **37**, 912.
14 K. Lee and M. A. El-Sayed, *J. Phys. Chem. B*, 2006, **110**, 19220.
15 J. E. Park, M. Atobe and T. Fuchigami, *Ultrason. Sonochem*., 2006, **13**, 237.
16 V. G. Pol, A. Gedanken and J. Calderon-Moreno, *Chem. Mater*., 2003, **15**, 1111.
17 K. Okitsu, M. Ashokkumar and F. Grieser, *J. Phys. Chem. B*, 2005, **109**, 20673.
18 C. Su, P. Wu and C. Yeh, *J. Phys. Chem. B*, 2003, **107**, 14240.
19 M. A. Ortega, L. Rodriguez, J. Castillo, V. Piscitelli, A. Fernandez and L. Echevarria, *J. Opt. A: Pure Appl. Opt*., 2008, **10**, 104024.
20 D. Werner, S. Hashimoto, T. Tomita, S. Matsuo and Y. Makita, *J. Phys. Chem. C*, 2008, **112**, 16801.
21 S. Yang, T. Zhang, L. Zhang, S. Wang, Z. Yang and B. Ding, *Colloids Surf., A*, 2007, **296**, 37.
22 K. Esumi, A. Suzuki, N. Aihara, K. Usui and K. Torigoe, *Langmuir*, 1998, **14**, 3157.
23 M. Meyre, M. Tréguer-Delapierre and C. Faure, *Langmuir*, 2008, **24**, 4423.
24 T. K. Sau, A. Pal, N. R. Jana, Z. L. Wang and T. Pal, *J. Nanopart. Res*., 2001, **3**, 257.
25 H. Chen, Y. Wang and S. Dong, *J. Raman Spectrosc*., 2009, **40**, 1188.
26 K. Mallick, M. J. Witcomb and M. S. Scurrell, *Eur. Phys. J.: Appl. Phys*., 2005, **29**, 45.
27 A. Alexandrov, L. Smirnova, N. Yakimovich, N. Sapogova, L. Soustov, A. Kirsanov and N. Bityurin, *Appl. Surf. Sci*., 2005, **248**, 181.
28 J. Gu, W. Fan, A. Shimojima and T. Okubo, *J. Solid State Chem*., 2008, **181**, 957.
29 S. Kundu and H. Liang, *Langmuir*, 2008, **24**, 9668.
30 F. Liua, Y. Chang, F. Koa and T. Chu, *Mater. Lett*., 2004, **54**, 373.
31 F. Liu, C. Ker, Y. Chang, F. Ko, T. Chu and B. Dai, *Jpn. J. Appl. Phys*., 2003, **42**, 4152.

32 J. Turkevich, P. C. Stevenson and J. Hillier, *Discuss. Faraday Soc.*, 1951, **11**, 55.
33 J. Kimling, M. Maier, B. Okenve, V. Kotaidis, H. Ballot and A. Plech, *J. Phys. Chem. B*, 2006, **110**, 15700; M. A. Uppal, A. Kafizas, T. H. Lim and I. P. Parkin, *New J. Chem.*, 2010, **34**, 1401.
34 G. Schneider and G. Decher, *Langmuir*, 2008, **24**, 1778.
35 J. Kimling, M. Maier, B. Okenve, V. Kotaidis, H. Ballot and A. Plech, *J. Phys. Chem. B*, 2006, **110**, 15700.
36 R. A. Oriani, *Acta Metall.*, 1964, **12**, 1399; B. Rodriguez-Gonzalez, P. Mulvaney and L. M. Liz-Marzan, *Z. Phys. Chem.*, 2007, **221**, 415.
37 M. K. Chow and C. F. Zukoski, *J. Colloid Interface Sci.*, 1994, **165**, 97.
38 P. Raveendran, J. Fua and S. L. Wallen, *Green Chem.*, 2006, **8**, 34.
39 S. Kumar, K. S. Gandhi and R. Kumar, *Ind. Eng. Chem. Res.*, 2007, **46**, 3128; S. Biggs, P. Mulvaney, C. F. Zukoski and F. Grieser, *J. Am. Chem. Soc.*, 1994, **116**, 9150.
40 C. L. Nehl and J. H. Hafner, *J. Mater. Chem.*, 2008, **18**, 2415.
41 W. Haiss, N. Thanh, J. Aveyard and D. Fernig, *Anal. Chem.*, 2007, **79**, 4215.
42 X. Liu, M. Atwater, J. Wang and Q. Huo, *Colloids Surf., B*, 2007, **58**, 3.
43 Y. Nagata, Y. Mizukoshi, K. Okitsu and Y. Maeda, *Radiat. Res.*, 1996, **146**, 333.

